Supplementary Information

Antarctic temperature at orbital timescales controlled by local summer duration

P. Huybers (phuybers@fas.harvard.edu) and G. Denton.

- Supplementary Notes and Figures
  - Coherence and phase analysis
  - Single Column Atmospheric Model (SCAM)
- References

1 Supplementary note: coherence and phase

1.1 Methods

We use a multi-taper method (refs. S1,S2) to estimate the coherence between climate proxy records and insolation. In particular, the climate proxy records are first linearly interpolated to a uniform spacing of 1 ka and the corresponding insolation intensity is calculated using the orbital solution of Berger and Loutre (ref. S3). Although estimation of the coherence and phase is straightforward (ref. S2), estimation of the uncertainty accompanying these estimates requires that the peculiarities of the time-series be accounted for.

Significance levels for the coherence statistic have been tabulated for the case of stationary bivariate Gaussian processes (ref. S4), but in the present context we are interested in the significance of the coherence between a red-noise climate signal and a narrow-band insolation signal, for which we are unaware of a theoretical treatment of the significance level. Thus, we resort to a Monte Carlo procedure to estimate the 95% significance level between climate proxies and changes in insolation intensity. The algorithm we use is to generate a random-walk sequence, $x(t+1) = x(t) + \eta$, where η is a random variable drawn from a Gaussian distribution and t indicates time measured in ka. The sequence is stepped forward for 350 individual 1000 year time-steps. The resulting time-series, $x(t)$, is expected to have a red-spectrum with a power-law slope of two. We then compute the coherence between x(t) and a deterministic insolation time-series, the insolation at 65°N on June 21st over the last 350,000 years. Similar coherence values would be obtained if any other day or latitude were selected for computing the insolation. This Monte Carlo process is repeated 10,000 times in order to gather sufficient observations by which to estimate the approximate 95% significance level. When we use four windows, 95% of the Monte Carlo trials resides below a coherence of 0.65 at the obliquity (1/41ka ± 1/200ka) and precession bands (1/21ka ± 1/200ka). As expected, this is a more stringent significance level than for the case of two white-noise signals, where the approximate 95% confidence level is 0.6 (ref. S4).

The age-models associated with the proxy time-series have been constructed to be consistent with an assumed orbital forcing curve. Thus, the coherence estimates are expected to be biased high. This is certainly the case for the $\delta O_2/N_2$ record from Dome F when

placed on the DFGT2006 age-model (ref. 7) and also holds, although to a lesser extent, for the Dome F and Dome C proxy records of atmospheric temperature. If the coherence is biased high, its statistical significance will be overestimated and the accompanying phase uncertainty will be underestimated, but this further complication has not be accounted for in our calculations.

The uncertainty associated with phase is also estimated using a Monte Carlo procedure. First, two white-noise signals are generated, $x(t)$ and $y(t)$, and their Fourier transforms are computed, yielding $\hat{x}(s)$ and $\hat{y}(s)$, where s indicates frequency. We have also accounted for age model uncertainty in the Monte Carlo procedure. The phase of $\hat{y}(s)$ is shifted in each realization in a manner consistent with a shift in time, $\hat{y}'(s) = \hat{y}(s) \exp -2\pi i\delta/s$, where the time shift, δ, is drawn from a zero-mean normal distribution having a standard deviation consistent with the age model uncertainty. The reported age-model uncertainty for Dome F is ± 0.75 ka (1σ, ref. S7) but may be larger. The Dome F age-model was in part estimated by aligning $\delta O_2/N_2$ observations with local changes in insolation (ref. 7), whereas the relationship between insolation and the $\delta O_2/N_2$ is itself uncertain (refs. 7,14). Age-model uncertainty for the Dome C ice-core is approximately ± 3 ka (1σ, ref. S5) and is treated in a manner analogous with the Dome F uncertainty. If the age-model error is not systematic, it will influence both the coherence and phase estimates. But additional Monte Carlo trials including this phenomena give results in keeping with the simpler systematic representation of age-model uncertainty, and such further complications are not pursued here.

The two signals, $\hat{x}(s)$ and $\hat{y}'(s)$, are combined into a third signal according to the degree of coherence, $\hat{z}(s) = \sqrt{1 - c(s)^2}\hat{x}(s) + c(s)\hat{y}'(s)$, where $c(s)$ is the bias-corrected coherence estimate (ref. S3). This bias correction is separate from the issues involving orbital tuning and, instead, addresses the fact that the expected value of the coherence estimate is positive even when the true coherence is zero. Finally, the phase is computed between $\hat{z}(s)$ and $\hat{y}(s)$ using the multi-taper coherence routine with four windows. This algorithm is repeated 10,000 times to estimate the width of the distribution of each phase.

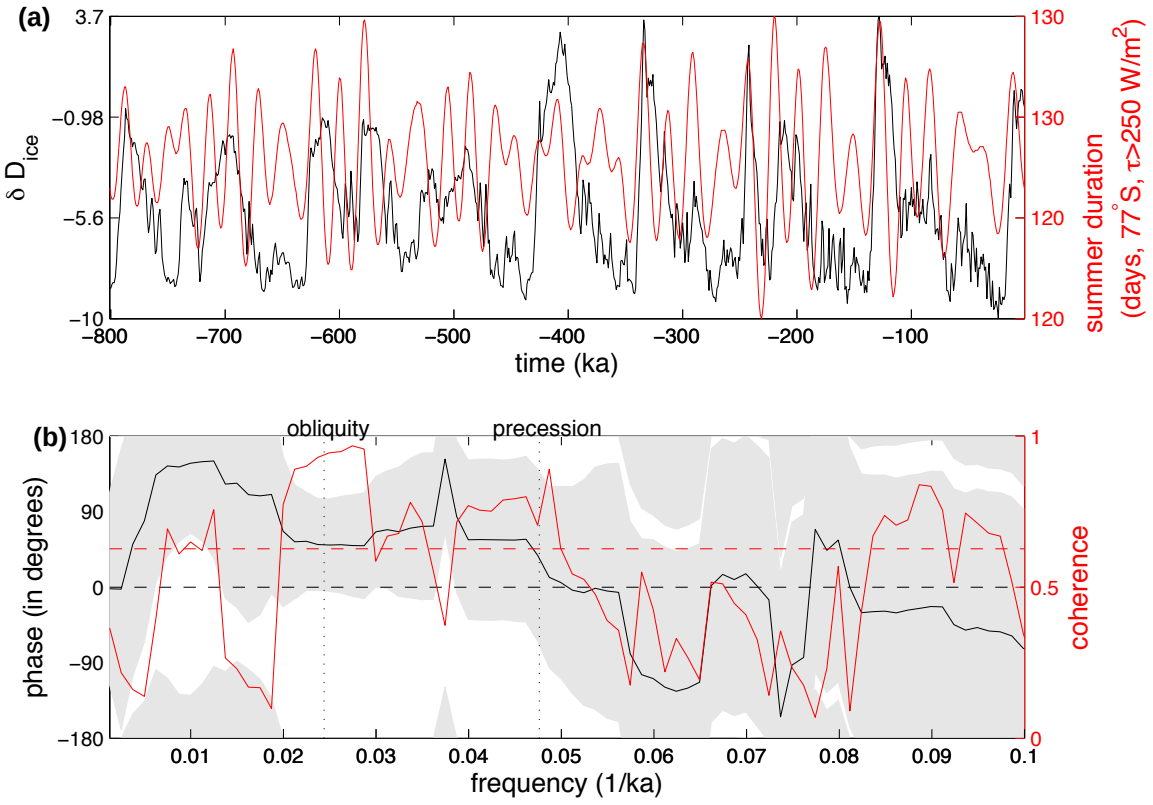

Figure 1: **The coherence and phase between the Dome C δD record and the duration of southern summer.** (a) Time-series of the Dome C δD proxy for mean annual temperature (ref. 6) and the duration of summer, measured as the number of days daily average insolation at 77°S exceeds a threshold of 250 W/m^2. (b) The coherence (red) and phase (black) between the two time-series. Positive phase indicates that the insolation leads. The approximate 95% confidence level for the coherence between red noise and a narrow-band signal is indicated by the red dashed line; the zero phase line is indicated by the black dashed line, and the approximate 95% confidence interval for phase is indicated by the gray shading. Phase uncertainty accounts for the ±3 ka age model uncertainty. Vertical dotted lines indicate the obliquity (1/41Ky) and precession (1/21Ky) bands.

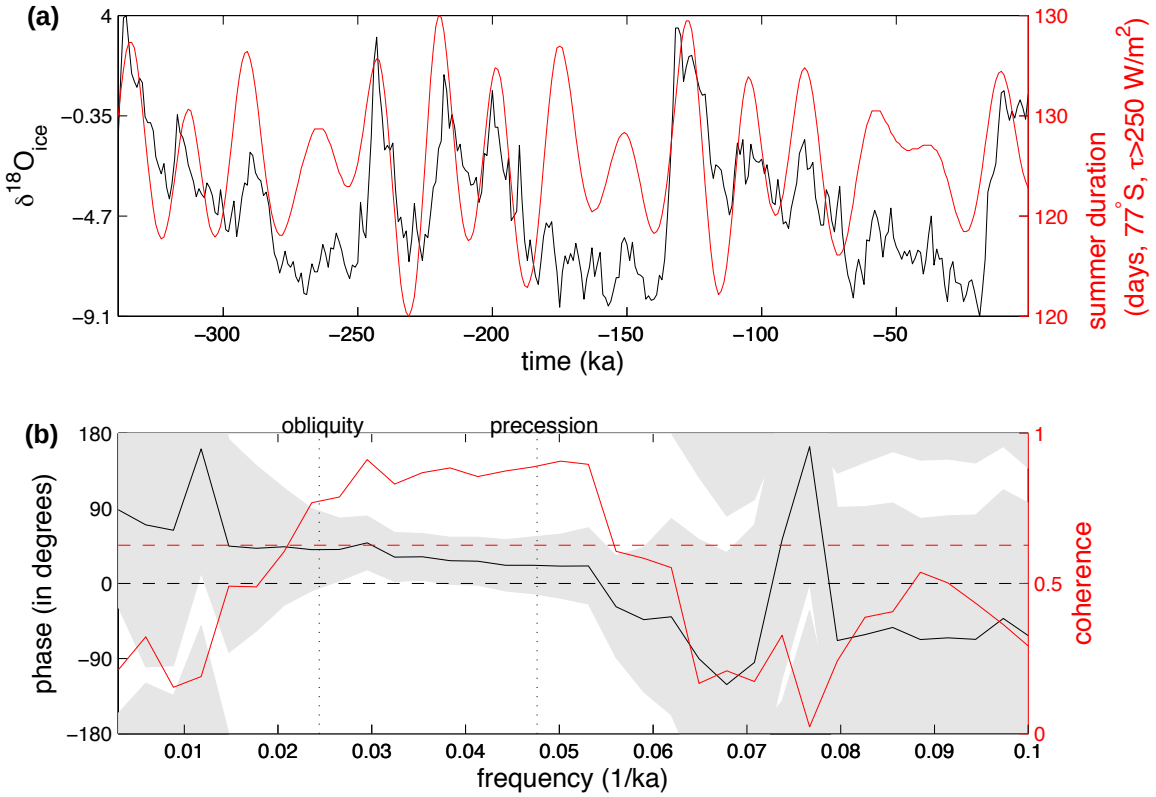

Figure 2: **The coherence and phase between the Dome F δ^{18}O record and the duration of southern summer.** The format follows that of fig. 1 and shows a similar coherence and phase at the orbital bands. An age-model uncertainty of ±0.75 ka is used in estimating the 95% confidence interval for the phase.

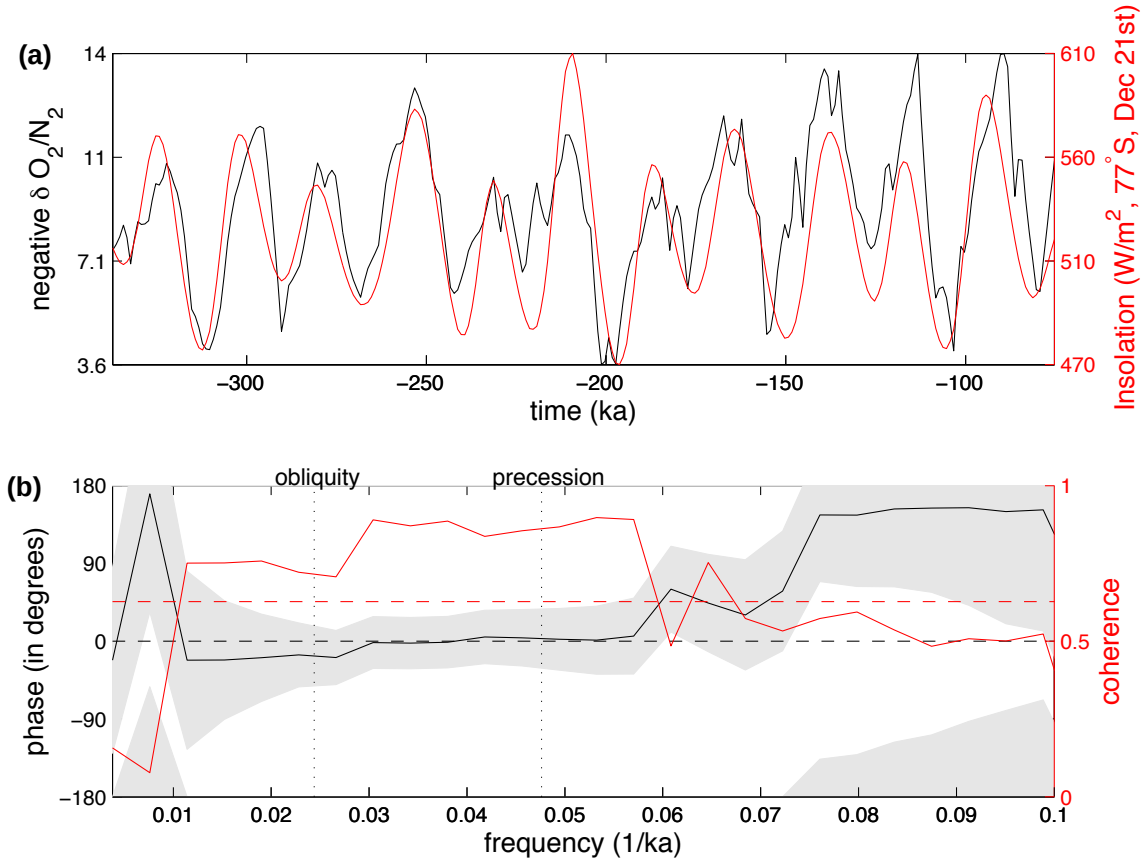

Figure 3: **The coherence and phase between the Dome F $\delta O_2/N_2$ record and summer insolation intensity** The format follows that of fig. 1, except that the negative of the $\delta O_2/N_2$ is plotted and used in the coherence and phase analysis. An age-model uncertainty of ± 0.75 ka is used in estimating the 95% confidence interval for the phase. Note that the high coherence and zero phase relationship is expected as the age model used in this analysis was tuned to summer insolation intensity (ref. 7).

1.2 Insolation compared against Dome F and Dome C proxy records

Here we discuss the coherence and phase between three ice-core proxy records and changes in insolation. The three records are the the Dome C atmospheric δD temperature proxy record on the EDC3 time scale (refs S5,6, Fig. 1), the Dome F atmospheric temperature proxy record on the DFO-2006 time scale (ref. 7, Fig. 2), and Dome F $\delta O_2/N_2$ also on the DFO-2006 time-scale (ref. 7, Fig. 3). All three records show significant coherence with insolation at the precession and obliquity bands. The coherence results are insensitive to changes in the latitude or the day of the year for which insolation is calculated (excluding polar night), or to whether duration or intensity is calculated. However, these choices as to how insolation is calculated do determine the phase.

The Dome F and Dome C ice-core proxy records of atmospheric temperature both indicate a lag with respect to northern insolation (77°N) on June 21st, but the uncertainties in phase are slightly larger than the lag. If the phase is computed using the intensity of Northern Hemisphere summer, instead of the duration of Southern Hemisphere summer, the resulting coherence and phase estimates are indistinguishable. The Dome F $\delta O_2/N_2$ is almost exactly in phase with changes in local (77°S) insolation on Dec. 21st. This is partly by construction, as the $\delta O_2/N_2$ chronology was tuned to this quantity (ref. 7).

The coherence between temperature in SCAM and insolation is nearly perfect ($c > 0.99$). The maximum seasonal surface temperatures (daily averages) are in phase with local insolation on Dec 21st, while the annual average atmospheric temperatures are in phase with local changes in the duration of the seasons and northern hemisphere insolation on June 21st. We do not show figures depicting these relationship as the extremely close correspondence among these records, as shown in Fig. 2, leaves little for additional figures to contribute.

2 Supplementary note: Single Column Atmospheric Model

More complete discussion and references regarding the Single Column Atmospheric Model (SCAM) can be found in ref. 22. We run SCAM in a standard configuration, and here

describe those details that are pertinent and peculiar to the model results reported in the main text. We specify SCAM to represent a location centered at 77°S and 40°E, near the Dome F ice core. The atmospheric CO_2 level is held at a constant 280 ppm, CH_4 at 600 ppb, and N_2O at 280 ppb. We also specify a constant latent-heat-flux convergence of 50 W/m^2 and a constant sensible heat-flux convergence of 100 W/m^2. The heat flux is distributed such that the seven lowest pressure levels, roughly corresponding to the troposphere below 400 mb, all warm by an equal increment at the end of each time step.

The sequence of model runs we perform is initiated at 350,000 years ago. We run the model forward for 25 years using a 20 minute step length. A seasonal equilibrium is apparently achieved within 10 years, but we run the model forward for 25 years to ensure equilibrium. We then advance the model date forward by 975 years and again run it to equilibrium over a period of 25 years. We continue in this fashion until reaching the present day, and report results averaged over the last five years of each individual model run. All model runs are identical, except that Earth's orbital configuration is adjusted at each interval. SCAMs radiation package calculates the changes in the top of the atmosphere shortwave insolation using the algorithm and orbital Fourier expansions published by Berger (ref. S6), which are consistent with more recent estimates of Earths orbit (ref. S3) over at least the last 500,000 years.

In order to explore the sensitivity of our results to changes in model parameterizations, we conducted a series of other runs. These alternate runs include a clear-sky configuration, a no-atmospheric-heat-flux convergence configuration, and a lower atmospheric CO2 (180 ppm) configuration. The same basic response to the orbital variations is observed in each of these modified scenarios, wherein a longer summertime leads to warmer annual average atmospheric temperature. Note that components of the model state including the vertical temperature structure, atmospheric water vapor content, and snow albedo are all dynamically calculated (e.g. refs. 22, 23). Thus the changes imposed in clouds, heat flux convergence, and CO2 also influence virtually every component of the model. To provide a specific example, snow albedo is calculated as a function of temperature (ref. S7) so that each alternate run of the model informs us about the model response to orbital variations in the presence of a different albedo. The important point is that although the atmospheric

temperature in the model is sensitive to a host of environmental factors, the mean annual atmospheric temperature in the model consistently follows the duration of the summer in the manner anticipated from radiative equilibrium. Thus, our model results support our hypothesis that radiative equilibrium processes give rise to at least part of the orbital period variability recorded in Antarctic ice core temperature proxies, even in the presence of a changing background climate.

We have also argued in the main text that mean annual atmospheric temperature above Antarctica is largely controlled by radiative equilibrium processes because of the peculiarities of the Antarctic climate. By extension, we do not necessarily expect that radiative equilibrium will dominate mean annual temperature away from Antarctica, and we test this inference by running SCAM at positions in the Tropical Atlantic and the Labrador Sea. The Tropical Atlantic run shows minimal change in annual average tropospheric temperature with orbital variations, while the Labrador Sea run indicates that temperature varies with Northern Hemisphere summer insolation intensity. Although more complete study of the various local responses to changes in insolation is warranted, these runs support the inference that Antarctic climate is peculiarly sensitive to changes in the duration of the seasons whereas Northern climate is more liable to be influenced by changes in the intensity of insolation. We anticipate that conditions similar to those above the Antarctic Ice Sheet today may have prevailed above the Laurentide Ice Sheet during the last glacial. However, because the Laurentide had significant surface ablation zones on land, as described in the main text, we expect that local radiative balance would have been secondary to ice-albedo feedbacks in controlling Laurentide atmospheric temperatures.

References

[1] Thomson, D. J. Time series analysis of Holocene climate data. *Philosophical Transactions of the Royal Society of London* **A 330**, 601–616 (1990).

[2] Percival, D. & Walden, A. *Spectral Analysis for Physical Applications* (Cambridge University Press, 1993).

[3] Berger, A. L. Astronomical theory of paleoclimates and the last glacial-interglacial cycle. *Quat. Sci. Rev.* **11**, 571–581 (1992).

[4] Amos, D. & Koopmans, L. *Tables of the Distribution of the Coefficient of Coherence for Stationary Bivariate Gaussian Processes*, vol. SCR-483 (Sandia Corp., 1962).

[5] Parrenin, F. *et al.* The EDC3 chronology for the EPICA Dome C ice core. *Climate of the Past* **3**, 485–497 (2007).

[6] Berger, A. Long-term variations of daily insolation and Quaternary climatic changes. *Journal of Atmospheric Sciences* **35**, 2362–2367 (1978).

[7] Briegleb, B. Delta-Eddington approximation for solar radiation in the NCAR community climate model. *Journal of Geophysical Research* **97**, 7603–7612 (1992).